dition. This indicated that the jump conditions at the surface might not be represented correctly with presently available models. Particular interest centered on various slip constants used in the preceding set of calculations, given as

$$a_l = 1.2304(2-\theta_r)/\theta_r$$

$$b_l = 1.1750(2-\theta_r)/\theta_r$$

$$c_l = 2.3071(2-\alpha_t)/\alpha_t$$

where θ_r = fraction of incident molecules diffusely reflected and α_t = thermal accommodation coefficient.

The possibility that the slip constants a_l, b_l, c_l did not represent the present flow correctly was explored in a numerical experiment to assess the sensitivity of the results to those values. Since the Stanton number was, in general, in close agreement with experiment, only the constants appearing in a_l and b_l (which directly influence the pressure level) were varied in the study. New constants were established which exactly correspond to a 40% increase in θ_r. However, since θ_r by nature should be unity or less, this result translates to the new set of coefficients, where the constants 1.2304 in a_l are replaced by 0.527 and 1.1750 in b_l by 0.505. Figure 1 shows excellent comparison of the experimental and numerical pressure distributions using the foregoing set of slip constants. It has been found that the change in the coefficients of the slip constants did not produce any loss in the good comparisons of the Stanton number.

Note is made here of the fact that there have been many efforts in the past to determine these constants by other authors. Figure 2 shows the predicted numerical results obtained here using the slip constants proposed by Payne,[5] Welander,[6] and Mott-Smith[4] in comparison with those established in the present analysis. Although all of these slip constants seem to yield the same results for downstream points, the slip constants in the present form show the correct trend of the experimental data at the stagnation point also.

Further comparisons were made with Little's data[15] for flow past a paraboloid over a range of freestream Reynolds numbers of 180 to 12,700 and a freestream Mach number of 10. The predicted results, shown in Fig. 3, compare well with the experimental data.

Based on the comparisons between the theoretical calculations and the experimental data presented here, it appears that the viscous shock layer model is accurate over the major portion of a blunt surface for a wide range of Reynolds numbers. The apparent discrepancy in the predicted surface pressure in the stagnation region apparently is attributable to the slip constants used to represent the higher-order Reynolds number effects at the surface. The constants established in this study seem to correct this deficiency.

References

[1] Cheng, H. K., "The Blunt-Body Problem in Hypersonic Flow at Low Reynolds Number," Rept. AF-1285-A-10, June 1963, Cornell Aeronautical Laboratory, Buffalo, N. Y.

[2] Jain, A. C. and Adimurthy, V., "Hypersonic Merged Stagnation Shock Layers. Part I. Adaibatic Wall Case," *AIAA Journal*, Vol. 12, March 1974, pp. 342-347.

[3] Sherman, F. A., "A Low Density Wind-Tunnel Study of Shock Wave Structure and Relaxation Phenomena in Gases," TN 3298, 1955, NACA.

[4] Mott-Smith, H. M., "A New Approach in the Kinetic Theory of Gases," Group Rept., V-2, Dec. 1954, Lincoln Laboratory, Massachusetts Institute of Technology, Cambridge, Mass.

[5] Payne, M., "Temperature-Jump and Velocity of Slip at the Boundary of Gas," *Journal of Chemical Physics*, Vol. 21, 1953, pp. 2127-2131.

[6] Welander, P., "On Temperature Jump in Rarefied Gas," *Arkiv fur Fysik*, Vol. 7, 1954, pp. 507-553.

[7] Cheng, S.-I, and Chen, J. H., "Slip, Friction and Heat Transfer Laws in a Merged Regime," *Physics of Fluids*, Vol. 17, Sept. 1974, pp. 1677-1687.

[8] Davis, R. T., "Numerical Solution of the Hypersonic Viscous Shock Layer Equations," *AIAA Journal*, Vol. 8, May 1970, pp. 843-851.

[9] Thyagaraja, A., "Compressible Flows at Small Reynolds Numbers," Ph. D. thesis, 1972, Department of Mathematics, California Institute of Technology, Pasadena, Calif.

[10] Blottner, F. G. and Flugge-Lotz, I., "Finite-Difference Computation of the Boundary Layer with Displacement Interaction," *Journal de Mecanque*, Vol. II, April 1963.

[11] Srivastava, B. N., Werle, M. J., and Davis, R. T., "Solution of the Hypersonic Viscous Shock Layer Equations for Flow Past a Paraboloid," Rept. AFL-74-4-10, April 1974, Department of Aerospace Engineering, University of Cincinnati, Cincinnati, Ohio.

[12] Davis, R. T. and Nei, Y. W., "Numerical Solution of the Viscous Shock Layer Equations for Flow Past Spheres and Paraboloids," Final Rept., Contract 48-9195, Sandia Corporation.

[13] Boylan, D. E., private communication, Aug. 1971, Aerodynamics Division, Von Karman Gas Dynamics Facility, Arnold Rsearch Organization, Arnold Air Force Station, Tenn.

[14] Davis, R. T., "Hypersonic Flow of a Chemically Reacting Binary Mixture Past a Blunt Body," AIAA paper 70-805, Los Angeles, Calif., 1970.

[15] Little, H. R., "Surface Conditions on Hyperboloids and Paraboliods in Hypersonic Flow," AIAA paper, 70-182, New York, N. Y. 1970.

Disjoint Design Spaces in the Optimization of Harmonically Excited Structures

Erwin H. Johnson*
NASA Ames Research Center, Moffett Field, Calif.

Nomenclature

G	= shear modulus (psi)
$I_{\alpha 0}$	= mass polar moment of inertia/thickness (slugs)
J_0	= area polar moment of inertia/thickness (in.^{3})
L	= length of the rod (in.)
R	= radius of the rod (in.)
S	= nondimensional spanwise coordinate
t_i	= thickness, design variable (in.)
$\bar{T}$	= amplitude of the applied torque (lb)
θ	= rotational displacement (rad)
λ	= nondimensional frequency ($= \omega^2 I_{\alpha 0} L^2 / (6GJ_0)$)
ω_e	= frequency of the harmonic excitation (rad/sec)

THE optimization of structures undergoing harmonic excitation serves as a valuable starting point for structural optimization studies with more general dynamic loadings. References 1-3 deal with the minimum weight design of one-dimensional structures under such conditions by developing optimality criteria based on energy methods. In these studies, equality constraints were placed on the amplitude of the displacement or on the dynamic compliance. It was also necessary to specify that the structure's first natural frequency of vibration be greater than the excitation frequency. This

Received July 11, 1975; revision received September 29, 1975. The author gratefully acknowledges the fellowship support he received from the Fannie and John Hertz Foundation while performing the research reported on in this Note.

Index categories: Structural Design, Optimal; Structural Dynamic Analysis.

*National Research Council Postdoctoral Fellow. Member AIAA.

Note removes the frequency constraint, replaces the displacement constraint by an inequality constraint on the allowable stress, and uses finite element approximations to the continuous one-dimensional structures. Such a formulation is felt to be of greater interest in the design of practical structures. When the question is posed in this manner, an interesting theoretical feature of these problems is revealed: the feasible design space is disconnected or "disjoint." This disjoint property was previously observed by Cassis[4] in the optimal design of frame structures subjected to half-cycle sine pulses, but the present Note offers a more complete physical explanation of the phenomenon.

Two Design Variable Example

This section considers the optimal design of a thin-walled cantilevered rod subjected to steady, simple harmonic, torsional excitation. The rod is modeled by two finite elements of equal length, with the thickness of these elements treated as the design variables. The stiffness and inertial properties are considered proportional to the thicknesses, an assumption which leads to the following equations for the amplitude of the response

$$\left[-\frac{\omega_e^2 I_{\alpha 0} L^2}{24 G J_0}\begin{bmatrix} 2(t_1+t_2) & t_2 \\ t_2 & 2t_2 \end{bmatrix} + \begin{bmatrix} t_1+t_2 & -t_2 \\ -t_2 & t_2 \end{bmatrix}\right]\begin{Bmatrix} \theta_1 \\ \theta_2 \end{Bmatrix} = \frac{\bar{T}L^2}{8GJ_0}\begin{Bmatrix} 2 \\ 1 \end{Bmatrix} \tag{1}$$

The constraints considered are that the stress magnitudes everywhere in the rod be less than a specified value, $\sigma_{\max}$. This condition is expressed by the formula

$$\left|\frac{1}{\sigma_{\max}}\begin{Bmatrix} \sigma_1 \\ \sigma_2 \end{Bmatrix}\right| = \left|\frac{2GR}{\sigma_{\max} L}\begin{bmatrix} 1 & 0 \\ -1 & 1 \end{bmatrix}\begin{Bmatrix} \theta_1 \\ \theta_2 \end{Bmatrix}\right| \leq \begin{Bmatrix} 1.0 \\ 1.0 \end{Bmatrix} \tag{2}$$

An additional "minimum gage" condition is that the design variables be greater than 0.04 in. ($t_i \geq 0.04$). The stress constraints can be evaluated for a given design condition by combining Eqs. (1) and (2) and specifying values for λ_e, the nondimensional excitation frequency, and for $\bar{T}LR/(4J_0\sigma_{\max})$. The latter parameter was set at 0.085.

The motivation for representing the structure by two design variables is that it is possible to depict the results graphically, thereby gaining a qualitative indication of what would be encountered with a more realistic representation using many design variables. Figures 1 and 2 show the design spaces for values λ_e equal to 1/6 and 2/3, respectively. The shaded portions of the figures bound areas where the designs are infeasible (i.e., some constraint is violated). The least weight solutions are at the points inside the feasible regions where (t_1+t_2) is at a minimum. For Fig. 1 this occurs at $t_1=0.33$ and $t_2=0.120$, while in Fig. 2 the optimum is at $t_1=0.04$ and $t_2=0.251$.

The disjoint character of the design space is demonstrated in the two figures by the division of the feasible design space into two unconnected regions. An explanation for this curious behavior is to be found by studying the natural frequencies of the system. The dashed lines of Figs. 1 and 2 represent the loci of points where the lowest natural frequency, λ_1, is equal to the excitation frequency. Designs that have $\lambda_1=\lambda_e$ are obviously infeasible because they are at a resonance condition, which, in the absence of damping, produces an unbounded response. The dashed line of Fig. 2 has the equation $t_1=2.06t_2$. The region $t_1>2.06t_2$ contains designs where $\lambda_1 \geq \lambda_e$, whereas the region $t_1<2.06t_2$ has $\lambda_1<\lambda_e$. Each of these regions contains its own optimum, as the figure shows.

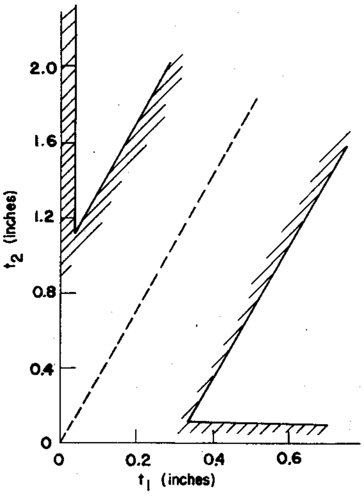

Fig. 1 Design space for $\lambda_e=1/6$.

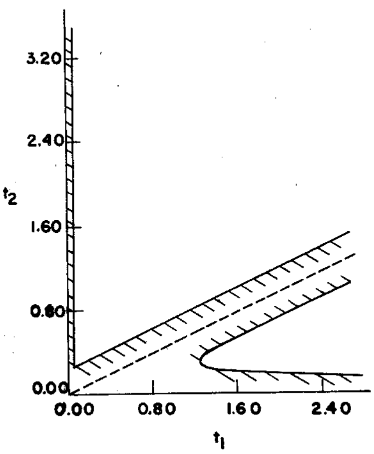

Fig. 2 Design space for $\lambda_e=2/3$.

Arbitrary Number of Design Variables

The previous section demonstrated that it is possible to thoroughly analyze the two design variable case graphically. With more numerous variables, graphical techniques become impractical and some method of numerical optimization must be used. This section briefly presents the results of the application of numerical methods to the optimization of a cantilevered rod identical to the rod of the previous section. Ten equal length elements were used in the analysis, rather than two. The disjoint nature of the design space is the primary complicating factor in the search for a least weight solution in that it creates the possibility of the existence of a number of local optima. An indication of this is given by Figs. 3 and 4, which show distinct optima for the present example for the same nondimensional excitation frequency of $\lambda_e=2/3$.

The result shown in Fig. 3 was obtained by the author[5] by means of an optimization algorithm using the variable metric method. The thickness distribution given in this figure has a first natural frequency that is greater than the excitation frequency. The distribution appears quite reasonable in that it is thickest at the root and tapers gradually to the tip.

Figure 4 shows the thickness distribution of a second optimum for this example that was obtained using a search

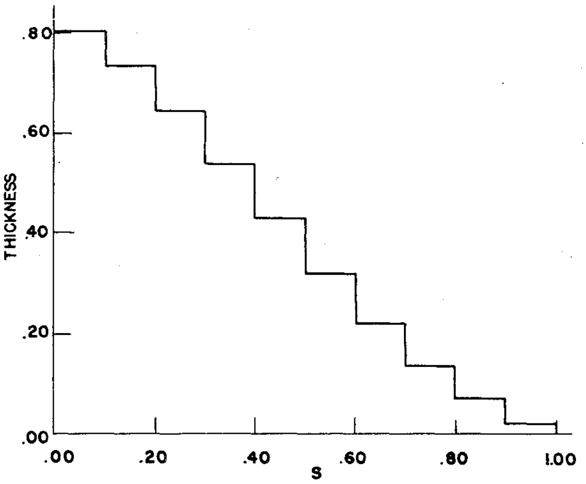

Fig. 3 Optimal thickness distribution with $\lambda_e < \lambda_1$.

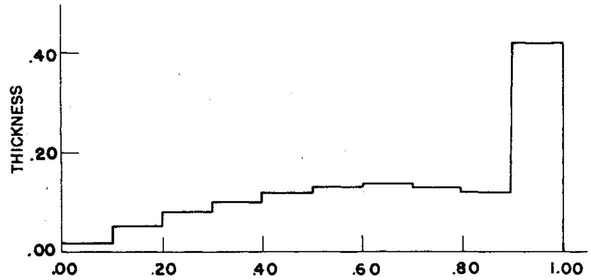

Fig. 4 Optimal thickness distribution with $\lambda_e > \lambda_1$.

algorithm designed by P. Rizzi.[6] This distribution has a first natural frequency that is less than the excitation frequency, indicating that this solution is in a feasible region unconnected from the feasible region associated with the distribution shown in Fig. 3. The thickness distribution of Fig. 4 is quite odd in that it has the minimum value specified at the root and has a large thickness concentrated near the tip. By studying the response of this structure, it can be shown that the effect of the large thickness near the tip is to create an inertial force that counteracts the applied load by acting out of phase with it. This tends to relieve the stresses throughout the structure.

The weight of the structures can be considered proportional to a factor equal to

$$\sum_{i=1}^{10} t_i/10$$

For the design of Fig. 3, this factor is 0.3932, while for Fig. 4, it is 0.1311.

Conclusions

This Note points out a novel and complicating feature in the study of structural optimization with harmonic or other dynamic excitation. In addition, an example is presented where the least weight solution is a design that is not intuitively reasonable. A number of questions relevant to the phenomenon of disjoint design spaces remain. Chief among these are the determination of the number of local optima that can exist for a given example and the development of an efficient method for seeking the various optima.

References

[1] Icerman, L.J., "Optimal Structural Design for Given Dynamic Deflection," *International Journal of Solids and Structures,* Vol. 5, May 1969, pp. 473-490.

[2] Plaut, R.H., "Optimal Structural Design for Given Deflection Under Periodic Loading," *Quarterly of Applied Mathematics,* Vol. 29, July 1971, pp. 315-318.

[3] Mroz, A., "Optimal Design of Elastic Structures Subjected to Dynamic, Harmonically Varying Loads," *Zeitschrift fur Angewandte Mathematik and Mechanik,* Vol. 50, May 1970, pp. 303-309.

[4] Casis, J.H., "Optimum Design of Structures Subjected to Dynamic Loads," UCLA-ENG-7451, June 1974, UCLA, School of Eng. and Applied Sci., Los Angeles, Calif.

[5] Johnson, E.H., "Optimization of Structures Undergoing Harmonic or Stochastic Excitation," Ph.D. thesis, May 1975, Chap. III, Stanford University, Stanford, Calif.

[6] Rizzi, P., "The Optimization of Structures with Complex Constraints via an Optimality Criterion Method," Ph.D. thesis, June 1976, Dept of Aeronautics and Astronautics, Stanford University, Stanford, Calif.

Analytical Model for a Two-Phase Vacuum Plume

Blaine E. Pearce*
The Aerospace Corporation, El Segundo, Calif.

Nomenclature

B	= constant
I_{sp}	= motor specific impulse
k	= constant in particle density equation ($k = 2.5$)
$\dot{m}$	= motor total mass flow rate
p	= pressure
r	= radial distance from exit plane
r^*	= nozzle throat radius
V	= velocity
$\bar{v}_p$	= average particle velocity
V_ℓ	= thermodynamic limiting velocity for the gas
ρ	= density
ξ	= nondimensional angular coordinate, $\xi = \phi/\phi_m$
ϕ	= azimuthal angle
ϕ_m	= limiting particle streamline angle
λ	= constant in gas density equation
ϵ	= nozzle exit area ratio
x_p	= mass fraction of solid particles
Subscripts	
p	= particle
g	= gas
o	= chamber conditions

I. Introduction

THIS Note describes an approximate analytical model for the two-phase (gas/solid particle) vacuum plume from a solid propellant rocket motor. It is applicable to motors with thrust levels from a few hundred to several thousand pounds utilizing propellants containing the nominal (30% by weight) mass fraction of aluminum oxide particles in the exhaust products. The model provides a simple, analytical description of the undisturbed plume structure valid far from the exit plane (more than about 10 exit radii) which has been found useful in assessing plume impingement effects. Although essentially exact flowfield solutions for these plumes can be obtained from numerical codes, the approximate analytical model has proved valuable in both preliminary and more detailed analyses. This is particularly true for erosion and contamination estimates for which the uncertainty in the plume/surface interaction mechanisms

Received August 6, 1975; revision received November 26, 1975.

Index categories: Multiphase Flows; Jets, Wakes, and Viscid-Inviscid Flow Interactions.

*Member of the Technical Staff, Aerothermodynamics Department. Member AIAA.